Structural Examination of the Influence of Phosphorylation on the Binding of Fibrinopeptide A to Bovine Thrombin†

Muriel C. Maurer,‡,§ Jin-Lin Peng,‖ Seong Soo An,‡ Jean-Yves Trosset,‡ Agnes Henschen-Edman,⊥ and Harold A. Scheraga*,‡

Baker Laboratory of Chemistry, and Cornell University Biotechnology Resource Center, Cornell University, Ithaca, New York 14853-1301 and Department of Molecular Biology and Biochemistry, University of California, Irvine, California 92697-3900

Received October 14, 1997; Revised Manuscript Received February 10, 1998

ABSTRACT: Upon addition of thrombin, fibrinopeptides A and B are cleaved off from the N-termini of four chains of fibrinogen $(A\alpha B\beta\gamma)_2$, and sites of polymerization are exposed, resulting in formation of a fibrin clot. For the fibrinogen Aα chain, cleavage occurs most prevalently at the Arg16−Gly17 peptide bond. About 25−30% of the human fibrinogen Aα chains are phosphorylated in nature at the position of Ser3, but the function for this modification is not understood. Previous NMR studies indicated that the N-terminal portion (^{1}ADSGE^5) of unphosphorylated fibrinopeptide A does not interact with the surface of bovine thrombin. Kinetic and NMR studies have now been carried out to assess whether phosphorylation at Ser3 allows the N-terminal segment (^{1}ADSGEGDFLAEGGGVR^{16}) to become anchored on the thrombin surface, leading to formation of a catalytically more efficient enzyme−substrate complex. Kinetic results indicate that phosphorylation leads to an approximately 65% increase in substrate specificity (k_{cat}/K_m) toward hydrolysis of fibrinogen Aα(1−20). ^{31}P NMR studies reveal that the phosphorylated group does interact with thrombin, and ^{1}H line broadening studies suggest that phosphorylation does promote binding of amino acids 1−5. Two-dimensional transferred nuclear Overhauser effect spectroscopy studies of bound fibrinopeptide A(1−16 Ser3P) indicate that phosphorylation allows new through-space interactions involving amino acid residues ^{1}ADSGE^5 to be observed. Computational docking of the peptide onto the X-ray structure of thrombin suggests that the phosphate may interact with basic residues at the rim of the heparin binding site of thrombin. As a result, the phosphate may serve as an anionic linker between the fibrinopeptide and the enzyme thrombin.

Fibrinogen is a plasma protein (MW 340 000) composed of three intertwining chains arranged into the dimer $(A\alpha B\beta\gamma)_2$. These chains are held in place covalently by a series of inter- and intrachain disulfide bonds (*1*). During the blood coagulation process, fibrinogen is converted to fibrin in three *reversible* steps (*2*). The serine protease thrombin hydrolyzes the N-terminal portions of the Aα and Bβ chains of fibrinogen to release two fibrinopeptide A and two fibrinopeptide B molecules, respectively (*3*−*10*). In human fibrinogen, hydrolysis occurs at the Arg16−Gly17 peptide bond of the Aα chain and at the Arg14−Gly15 peptide bond of the Bβ chain. Removal of the fibrinopeptides then leads to exposure of fibrin polymerization sites that react to form a resilient insoluble blood clot. Factor XIIIa helps stabilize the structure by introducing intermolecular γ-glutamyl-ε-lysine cross-links between the fibrin molecules (*11*−*16*).

The Aα chain of fibrinogen can be phosphorylated at the Ser3 (*17*) and Ser345 (*18*) positions. Various kinases have been screened for their ability to cause this modification of fibrinogen. From this screening work, some additional phosphorylation sites in the C-terminal regions of the Aα chain, which are not observed in nature, have been reported. The Aα chain can be phosphorylated in vitro by protein kinase C (*19*), protein kinase A, c-AMP dependent kinase, and casein kinases I and II (*19*−*21*). The identities of candidates for in vivo kinases continue to be investigated (*22*, *23*).

Under certain physiological and pathophysiological conditions, increased levels of phosphorylation have been observed in humans (*23*, *24*). For example, the extent of phosphorylation of human fetal fibrinogen is twice that of adult fibrinogen (*25*). In another example, the amount of phosphorylated fibrinogen has been reported to double within 24 h following hip replacement surgery (*18*).

Phosphorylation in the middle and C-terminal regions of the Aα chains may also affect the fiber characteristics of fibrin. Both increases and decreases in fiber thickness have been reported, depending upon the serines modified and the kinases employed. Phosphorylation of fibrinogen has also been reported to lead to a decrease in the rate of fibrin

† This work was supported by a research grant from the National Heart, Lung, and Blood Institute of the National Institutes of Health (Grant HL-30616). Support was also received from the Cornell Biotechnology Resource Center. M.C.M. was an NIH Postdoctoral Fellow, 1992−1995.

* To whom correspondence should be addressed.

‡ Baker Laboratory of Chemistry, Cornell University.

§ Present address: Department of Chemistry, University of Louisville, Louisville, Kentucky 40292.

‖ Cornell University Biotechnology Resource Center.

⊥ University of California.

S0006-2960(97)02538-5 CCC: $15.00
Published on Web 04/09/1998

degradation by plasmin (*19*, *21*, *26*, *27*). In addition, phosphorylation of fibrinogen may influence the ability of factor XIIIa to form cross-links between fibrin chains. This hypothesis has been proposed because phosphorylated Ser345 is located near Gln328 and Gln366, two residues known to participate in fibrin cross-linking sites (*18*).

The physiological function of phosphorylation at the Ser3 position of the FbgAα[1] chain is not known. The presence of a phosphate on this serine was first identified and characterized by Blomback et al. in 1962 (*17*). Of all the serines available on the Aα chain, Ser3 is the one most often phosphorylated, and the modification is found in 25−30% of the human fibrinogen Aα chains (*9*, *28*). Reverse-phase HPLC methods for isolating fibrinopeptides released upon thrombin hydrolysis of fibrinogen were developed in the early 1980s (*29*, *30*). These HPLC methods have been used successfully to identify and elucidate the source of various fibrinogen-based bleeding disorders (*31*, *32*). They have also been used in kinetic studies to map the residues of the substrate that are needed to produce an efficient enzyme−substrate complex (reviewed in refs *15* and *33*).

Using a mammalian system developed to overexpress human fibrinogen in Chinese hamster ovary (CHO) cells, Binnie et al. (*34*) demonstrated that the recombinant fibrinopeptide A (FpA), released by thrombin upon hydrolysis of the Aα chain, is phosphorylated to a degree similar to that seen in plasma-derived fibrinogen. This observation suggests that partial phosphorylation of fibrinogen occurs during biosynthesis and stands in contrast to previous proposals that all fibrinogen is phosphorylated and that FpA results from dephosphorylation of FpA-P (*17*, *35*). It appears, however, that the degree of phosphorylation is species-dependent. For example, canine FpA is phosphorylated to over 70%, whereas bovine FpA does not exhibit this modification at all (*28*, *35*, *36*).

Phosphorylation at the serine 3 position of the human fibrinogen Aα chain may moderate interactions between this chain and thrombin. Kinetic studies of unphosphorylated fibrinogen indicate that residues within positions 7−16 are most critical for thrombin activity (*15*, *16*). Further, one-dimensional proton line broadening NMR experiments reveal that amino acids 1−5 do not come in contact with the surface of thrombin (*37*). By contrast, Hanna et al. (*38*) reported that phosphorylated fibrinogen Aα exhibits a lower value of K_m toward thrombin than the unphosphorylated chain, whereas the value of k_{cat} is unaffected. They postulated that the phosphorylated serine may allow the complete FbgAα N-terminal sequence to interact with the surface of thrombin, producing a catalytically more efficient enzyme−substrate complex.

Here, we report a further exploration of the effects of phosphorylation on the binding of synthetic, human FbgAα-like peptides to thrombin. Kinetic studies indicate that phosphorylation at the serine 3 position of FbgAα(1−20) plays a role in increasing substrate binding to thrombin but has no effect on the turnover rate. One-dimensional line-broadening experiments involving ^{31}P and ^{1}H NMR indicate that phosphorylation promotes binding of FbgAα(1−5) to thrombin. Two-dimensional transferred NOESY studies, together with molecular modeling procedures, further suggest that phosphorylated FbgAα(1−6) has a conformation that enables it to bind to thrombin. This N-terminal segment has the potential for interacting with residues in the heparin binding site region of thrombin.

EXPERIMENTAL PROCEDURES

Materials. Bovine plasma barium citrate eluate (containing factors II, VII, IX, and X), *Echis carinatus* snake venom, and bovine fibrinogen (fraction I, type I) were all purchased from Sigma. PPACK (H-D-Phe-Pro-Arg chloromethyl ketone) was obtained from Bachem, whereas S2238 (H-D-phenylalanyl-L-pipecolyl-L-arginine *p*-nitroanilide) was obtained from Kabi Pharmacia. For all NMR experiments, HPLC-grade *o*-phosphoric acid (85%, Fisher) and 99.9% D_2O (Cambridge Isotope) were used.

Synthesis of Peptides. Peptides based on residues 1−20 of the human fibrinogen Aα chain were synthesized by solid-phase methodologies at the Cornell University Biotechnology Resource Center and at the University of California Irvine Peptide Synthesis Facility. The amino acid sequences of the unphosphorylated and phosphorylated peptides are as follows: FbgAα(1−20), NH_3^+-ADSGEGDFLAEGGGVRG-PRV-COOH; FbgAα (1−20 Ser3P), NH_3^+-ADS(phos)-GEGDFLAEGGGVRGPRV-COOH. The phosphorylated and unphosphorylated peptides were prepared by solid-phase synthesis carried out on a Milligen 9050 peptide synthesizer using the Fmoc/tBu protection strategy. For the phosphorylated peptide, Ser was incorporated as side-chain-free Fmoc-Ser-OH. Phosphorylation was later achieved by treating the entire dry protected peptide with di-*tert*-butyl-diethylphosphoramidite/1*H*-tetrazole (*39*) followed by *tert*-butyl hydroperoxide oxidation (*40*). The phosphopeptide was purified by preparative RP-HPLC using a Waters Prep Nova-Pak HR C_{18} 6 μM 60 Å (25 mm × 100 mm) PrePak column on a Waters 625LC system and eluted with a linear gradient of 5−60% acetonitrile in 0.1% TFA over the course of 50 min. The fractions corresponding to the major peak were collected and lyophilized. The purified peptide showed a single peak both by analytical RP-HPLC on a YMC ODS-AQ column and by capillary electrophoresis on an ABI 270A system run with 1 M (trimethylammonium)propanesulfonate in 25 mM citric acid, pH 2.5. The MALDI-TOF mass spectrum of the peptide gave a molecular ion *m*/*z* of 2027.2 in the positive mode (theoretical value 2027) as measured by a Laser Mat 2000 (Finnigan Mat) mass spectrometer. The hydrolysis and amino acid analysis showed the expected molar ratios. Analytical RP-HPLC and capillary electrophoresis were also used to verify the purity of the unphosphorylated peptide. Mass spectrometry revealed a molecular ion *m*/*z* of 1947.8 (theoretical value 1946.1).

[1] Abbreviations: FbgAα, fibrinogen Aα; Ser3P, serine 3 phosphorylated; FpA, fibrinopeptide A; FpA-P; phosphorylated fibrinopeptide A; FpB, fibrinopeptide B; PEG, poly(ethylene glycol); S2238, H-D-phenylalanyl-L-pipecolyl-L-arginine *p*-nitroanilide; PPACK, H-D-Phe-Pro-Arg chloromethyl ketone; RP-HPLC, reverse-phase high-performance liquid chromatography; MUGB, methylumbelliferone guanidinobenzoate; K_m and k_{cat}, Michaelis−Menten kinetic constants; CHO cells, Chinese hamster ovary cells; NMR, nuclear magnetic resonance; NOESY, nuclear Overhauser effect spectroscopy; TR-NOESY, transferred nuclear Overhauser effect spectroscopy; TOCSY, total correlated spectroscopy; DQCOSY, double quantum filtered shift correlated spectroscopy; TFA, trifluoroacetic acid; DPFGSE, double pulsed-field gradient spin−echo; EM, energy minimization; SA, simulated annealing; MALDI-TOF, matrix-assisted laser desorption ionization-time-of-flight.

Peptides FbgAα(1−16) (or FpA) and FbgAα(1−16, Ser3P) (or FpA-P) were obtained by thrombin digestion of the purified FbgAα(1−20) and (1−20, Ser3P) peptides, respectively. In a typical experiment, a mixture of 5 mg of peptide and 0.5 μM thrombin in 50 mM H_3PO_4 (pH 6.3), 300 mM NaCl, and 0.01% PEG 8000 was incubated for 6−12 h at 37 °C. The reaction was quenched upon addition of H_3PO_4 to a final concentration of 5%. The mixture was loaded on a Kromosil KR 100−5 C_{18} (250 × 10 mm) column equilibrated at 5% acetonitrile/0.09% TFA. Hydrolyzed peptide was eluted with a gradient of 5−70% acetonitrile in 0.09% TFA over the course of 45 min. The identity and purity of the hydrolyzed peptides were verified by MALDI-TOF mass spectrometry and by quantitative amino acid analysis using Waters Pico-Tag chemistry. Under the conditions employed for these experiments, hydrolysis occurred only at the Arg16−Gly17 peptide bond. No hydrolysis products from cleavage at the minor Arg19-Val20 site were observed in the peak collected for 1−16.

Preparation of Bovine Thrombin. Bovine thrombin was isolated and purified by methods similar to those of Ni et al. (*37*). Bovine plasma barium citrate eluate (Sigma) was dissolved to a concentration of 80 mg/mL in 50 mM Tris, 150 mM NaCl, and 0.1% PEG 8000, pH 8 (activation buffer). Low molecular weight contaminants were removed by running the sample over a Pharmacia PD-10 column (Sephadex G25 resin) equilibrated with activation buffer. The eluted protein was then diluted to a final concentration of 10 mg/mL with the same buffer. $CaCl_2$ (10 mM) and *Echis carinatus* snake venom (0.1 mg/mL) were added, and the mixture was allowed to incubate for 50 min at 37 °C. The solution was then tested for the ability of thrombin to clot fibrinogen. The mixture was diluted 1:10 into a solution composed of 50 mM H_3PO_4, pH 8, 1 mg/mL BSA, 0.1% PEG, 100 mM NaCl, and 0.5 mg/mL bovine fibrinogen, and fibrin tendrils appeared within 20 s. The thrombin-containing mixture was next desalted on a 70 mL Sephadex G25 (Sigma) column into 25 mM H_3PO_4 (pH 6.5) and 100 mM NaCl. The resultant thrombin was subsequently purified on a Mono S column (HR 5/5) (Pharmacia) equilibrated with 25 mM H_3PO_4 (pH 6.5) and run on an LKB 2147 HPLC pump system with an LKB detector. After loading the enzyme mixture, the column was washed with the buffer mentioned above. A linear gradient running at 1 mL/min was implemented from 0 to 150 mM NaCl in 5 min, followed by a gradient from 150 to 400 mM NaCl in 50 min. The peak fractions for thrombin were pooled and then concentrated using an Amicon ultrafiltration stirred cell equipped with an Amicon YM-10 membrane (10 000 MW cutoff).

The concentration of protein was determined by using an extinction coefficient $E^{1\%} = 19.5$ at 280 nm (*41*). The purity of the isolated bovine thrombin was verified by SDS−PAGE. Thrombin aliquots at concentrations of approximately 100 μM were stored at −70 °C for future NMR studies. Some of the enzyme was also diluted to aliquots of 10 μM and 1 μM with 25 mM H_3PO_4 (pH 6.5), 300 mM NaCl, and 1 mg/mL bovine serum albumin (BSA) and kept for kinetic experiments. BSA was included to minimize adsorption of diluted enzyme onto the surface of the storage tubes.

Preparation of PPACK-Thrombin. Active-site-inhibited thrombin was prepared by incubating the enzyme with a 2-fold excess of PPACK. The reaction was carried out at 37 °C and was allowed to continue until thrombin could no longer hydrolyze the synthetic chromogenic substrate S2238. Excess PPACK reagent was removed by buffer exchange into NMR buffer (25 mM H_3PO_4 pH 5.6, 150 mM NaCl, and 0.2 mM EDTA) using an Amicon Centricon-10 ultrafiltration unit run in a Beckman JA-20 rotor spun at 6000 rpm in a Beckman Model J2-21 centrifuge. Any remaining unreacted PPACK was less than 5% of the total protein concentration.

MUGB Assay. The active-site concentration of thrombin was determined by titration with methylumbelliferone guanidinobenzoate (MUGB) using a Perkin-Elmer MPF-44B fluorescence spectrophotometer (*42*). The bovine thrombin used for NMR and kinetic studies was found to be greater than 95% active toward MUGB.

Kinetics of Hydrolysis of Fibrinogen Aα-like Peptides. Experiments to compare the initial velocity of thrombin-induced cleavage of FbgAα(1−20) vs FbgAα(1−20 Ser3P) were carried out using an HPLC assay. Thrombin was incubated at 25 °C with various concentrations of peptide. At specified times, an aliquot of the reaction mixture was quenched with 12.5% H_3PO_4, and the reaction products were run on an RP-HPLC column. Peak areas of the hydrolyzed products were converted to concentrations using a standard peptide calibration curve. The HPLC runs were carried out on a Brownlee Aquapore RP-300 7 μm, C_{18} column using an LKB 2147 HPLC pump system, 2157 LKB autosampler, 2221 LKB integrator, and a Gilson detector. Absorbance was measured at 215 nm. The mobile-phase buffers were A, 0.09% TFA in water, and B, 0.06% TFA in acetonitrile.

Standard peptide calibration curves over the range of 0−100 μM were prepared for FbgAα(1−16) and FbgAα-(1−16 Ser3P). Dilutions were made from stock solutions whose concentrations were assessed earlier by quantitative amino acid analysis. Aliquots were injected onto the Aquapore column and eluted at 0.5 mL/min using a gradient of 5−40% acetonitrile in 30 min for FbgAα(1−16) and a gradient of 5−45% acetonitrile in 45 min for FbgAα(1−16 Ser3P). All calibration curves were linear.

Kinetic experiments to characterize hydrolysis of the two peptides by thrombin were carried out at 25 °C in a buffer composed of 25 mM H_3PO_4 (pH 6.3), 300 mM NaCl, and 0.1% PEG 8000. Initial velocity measurements were made at this pH for the following reasons. The pH chosen should be similar to that used for the NMR studies (pH 5.6) but still allow for reasonable hydrolysis of the fibrinopeptides. Thrombin can hydrolyze fibrinogen Aα-like peptides at pH 5.6; however, the rate is greatly diminished from that at higher pH. The pH chosen should also not be too basic to prevent the release of the phosphate group and resulting formation of dehydroalanine, an analogue of alanine with a double bond between the C^{α} and C^{β} carbons. As a result of these requirements, a pH value of 6.3 was selected for the kinetics experiments, and mass spectrometry verified that the phosphate remained bound throughout the kinetic experiments.

In a typical kinetics experiment, 475 μL of reaction mixture was prepared with the desired concentration of peptide in 25 mM H_3PO_4 (pH 6.3), 300 mM NaCl, and 0.01% PEG 8000. The sample temperature was brought to 25 °C using a Labline Multi-Blok heating block. The reaction was started by adding 25 μL of 0.1 μM thrombin,

thus providing a final enzyme concentration of 5 nM. At specified time intervals, 75 μL of the reaction mixture plus thrombin was removed and quenched by adding it to an Eppendorf tube already containing 15 μL of 12.5% H_3PO_4. By use of the LKB autosampler, 30 μL aliquots were injected onto the Aquapore column. The column was washed for 15 min with 5% acetonitrile in TFA and eluted with the same gradient as used for the standard curves. Peaks for product FbgAα(1−16) and unhydrolyzed FbgAα(1−20) were observed. The extent of hydrolysis was generally 4−8%. Plots were generated for concentrations of hydrolyzed product vs time. The slopes of the straight lines correspond to initial velocities of peptide cleavage. Substrate concentrations were examined up to 1 mM. Buffering capacity was difficult to maintain at higher concentrations of peptides, and the results could not be well compared with values obtained at the lower concentrations. Kinetic parameters were determined by linear least-squares fit to the Hanes−Woolf plot using LINFIT (*43*) and the SigmaPlot program (Jandel Scientific Software, San Rafael, CA). In addition, data were evaluated by nonlinear regression analysis of the equation $V = V_{max}/\{1 + (K_m/[S])\}$ using the Marquardt−Levinthal algorithm (*44*) in the SigmaPlot program.

NMR Measurements: (A) Experimental Conditions. In preparation for each individual NMR experiment, a 100 μM aliquot of thrombin in 25 mM H_3PO_4 (pH 6.5) and 300 mM NaCl was defrosted and then buffer-exchanged into 25 mM H_3PO_4 (pH 5.6), 150 mM NaCl and 0.2 mM EDTA by use of a Centricon-10 ultrafiltration device. When working with thrombin, care had to be taken not to lower the pH below 5.3 since, under these conditions, the thrombin−peptide complex tended to precipitate. To minimize the risk of precipitation problems, peptide stock solutions were prepared at pH 6.0 and a small aliquot was added to the enzyme solution at pH 5.5−5.6. The pH was checked with a Beckmann Futura Plus electrode without correction for the presence of D_2O, which had been added to serve as a deuterium lock. By use of this procedure, little if any change in final pH occurred. Typically 50 μL of peptide solution was added to 350 μL of enzyme solution and the final D_2O concentration was 10%. As an example, 50 μL of a 14 mM peptide stock solution was added to 350 μL of a 170 μM thrombin stock solution providing a mole ratio of 12:1 of peptide to thrombin. To accommodate the small sample volume, Shigemi (BMS-005V) NMR tubes were employed.

All proton NMR experiments were conducted on a Varian Unity 500 MHz spectrometer equipped with a triple-resonance probe and pulsed-field *z*-gradients. The samples contained peptides at concentrations at a 10−15-fold molar excess over that of the thrombin. The water signal was suppressed either by presaturation or by the double pulsed-field gradient spin−echo (DPFGSE) technique developed by Hwang and Shaka (*45*).

The chemical shift assignments for the peptides were determined by TOCSY (τ_{mix} = 46 and 64 ms), NOESY, and DQCOSY experiments using the methods of Wüthrich (*46*). Chemical shifts were referenced against DSS at 0.0 ppm and against the HOD value at 4.80 ppm. Assignments referenced to HDO were in good agreement with those obtained earlier by Ni et al. (*47*) for FbgAα(1−20). A complete listing of the chemical shifts for FbgAα(1−20 Ser3P) can be found in Table 1. Chemical shift assignments were also made for FbgAα(1−20), FbgAα(1−16), and FbgAα(1−16 Ser3P) (data not shown).

Table 1: Proton Resonance Assignments[a] for Free FbgAα(1−20 Ser3P) in Aqueous Solution

residue	NH	$C^{\alpha}H$	$C^{\beta}H$	others
A1			1.55	
D2	8.80	4.67	2.68, 2.80	
S3	8.93[b]	4.52	4.14[c]	
G4	8.60	4.00		
E5	8.26[d]	4.33	2.07, 2.12	H^{γ} 2.31
G6	8.46	3.91		
D7	8.21	4.59	2.53, 2.64	
F8	8.17	4.57	3.14, 3.08	H^{δ} 7.28, H^{ϵ} 7.38, H^{ξ} 7.36
L9	8.13	4.27	1.60	H^{γ} 1.53, H^{δ} 0.90
A10	8.17	4.25	1.41	
E11	8.39	4.28	2.07, 1.98	H^{γ} 2.30
G12	8.46	3.96, 4.03		
G13/G14	8.31	3.97		
V15	8.06	4.12	2.08	H^{γ} 0.93
R16	8.50[e]	4.40	1.77, 1.88	H^{γ} 1.66, H^{δ} 3.20, H^{ϵ} 7.13
G17	8.26	4.05, 4.15		
P18		4.45	1.93, 2.01	H^{γ} 2.27, H^{δ} 3.64
R19	8.50	4.40	1.77, 1.88	H^{γ} 1.66, H^{δ} 3.20, H^{ϵ} 7.13
V20	7.76	4.06	2.08	H^{γ} 0.88

[a] Chemical Shift (parts per million) at pH 5.6 [referenced against DSS, 0.0 ppm]. [b] The NH chemical shift of S3 moves from 8.65 to 8.93 upon phosphorylation. [c] The chemical shift for the $C^{\beta}H$ of Ser 3 moves from 3.96 to 4.14 upon phosphorylation. [d] The chemical shift for NH of Glu5 moves from 8.33 to 8.26 upon phosphorylation. [e] The chemical shift for NH of Arg16 moves from 8.50 to 8.05 following hydrolysis.

(B) Transferred NOESY and 1D Proton Line Broadening. Transferred nuclear Overhauser effects allow transfer of information concerning relaxation between two nuclei in the bound ligand to the free ligand by means of chemical exchange (*48*−*50*). Sizable transferred NOEs are observed when the ligand molecule can associate/dissociate at least a few times during the NOE mixing time. Small, unstructured peptides free in solution generally do not exhibit any long-range NOEs. Upon introduction of less than stoichiometric amounts of enzyme, a number of NOEs corresponding to the bound structure of the peptides can be observed. These NOEs, which are large and negative, are a direct result of the considerable increase in rotational correlation time for the peptide in the bound state (*51*, *52*). Interactions between the peptide and the enzyme may also be monitored by 1D proton line broadening. Atoms of the peptides that come in direct contact with the enzyme surface experience changes in transverse relaxation time and chemical shift position. The resultant changes in line width/line shape and chemical shift position reflect weighted contributions of bound structure transferred to the free population.

Two-dimentional transferred NOESY (TR-NOESY) experiments were carried out using the standard NOESY pulse sequence and incorporating the DPFGSE solvent suppression method. Spectra were acquired with mixing times of 50−400 ms at 25 °C and with a mixing time of 250 ms at 10 and 15 °C. A gradient pulse was applied at the end of the mixing time for 2 ms at an amplitude of 7.8 G/cm. For each 2D NMR experiment, 32 transients of 2048 complex points/transient were obtained for each of 512 t_1 increments. Spectral width was 5999.7 Hz.

FbgAα(1−20) and FbgAα(1−20 Ser3P) were hydrolyzed by thrombin (during the NMR experiment) to produce

peptides 1−16 and 1−16 Ser3P, respectively. Transferred NOEs were not observed for the released tetrapeptide GPRV. This effect was further verified by the fact that there were no differences in the NMR results obtained for thrombin in the presence of either peptides 1−20 or 1−16.

(C) Phosphorus NMR. ^{31}P NMR spectra were collected on a Varian VXR-400 S spectrometer at 161.871 Hz with 128 transients and 16 000 points for the phosphopeptide and enzyme−phosphopeptide complexes. The H_3PO_4 present in the NMR buffer was used to standardize the chemical shifts. For the spectra, chemical shift position and line width were monitored. Chemical shift changes may occur for a ligand in response to a new environment and/or to a new bound conformation. Factors that influence the phosphorus chemical shift include bond geometry, electronegativity of substituents, and amount of π bonding. A change in the ionization state of the ligand may affect any one of these properties (*53*). The line width of the ^{31}P NMR peaks may be used to evaluate the chemical exchange properties of the enzyme−ligand complexes. Measurements were made in the range of pH 2.2−7.4 for the phosphopeptide and pH 5.6−7.0 for the enzyme−phosphopeptide complexes. As was used for the proton NMR studies, the samples contained peptides at concentrations at a 10−15-fold molar excess over that of thrombin.

Structure Calculation Procedure for Determining the Bound Conformation of FbgAα(1−16 Ser3P). Structure calculations were carried out using the X-PLOR 3.1 program (*54*) on the IBM SP2 supercomputer of the Cornell Theory Center to obtain the conformation of the isolated peptide in the conformation that it adopted when bound to thrombin. The molecular graphics program InsightII (Molecular Simulations Inc.) was used to visualize the resultant structures. The intensities of the transferred NOESY cross-peaks from a 250 ms experiment were categorized as weak, medium, and strong and converted to the following distance-constraint limits. The lower-bound distance values were all set to 1.8 Å. The upper-bound distance values were set to 2.6 ± 0.25 Å (strong), 3.3 ± 0.25 Å (medium), or 4.8 ± 0.25 Å (weak). A range of distances from 1.8 Å to the specified upper-bound values was therefore covered for each cross-peak classification. Eighty-three ^{1}H NOE distance constraints were used to describe the bound conformation of FbgAα(1−16 Ser3P). The phosphate on serine 3 of the fibrinopeptide was also included in the structure calculation procedure. Bond lengths, bond angles, dihedral angles, and partial charges for this group were taken from the phosphate present in the X-PLOR DNA topology and parameter files. This phosphate unit was generated as part of a complete amino acid residue and added to the topology and parameter files of serine, i.e., a new residue *serp* was created and incorporated into the X-PLOR sequence file for FbgAα(1−16 Ser3P).

Throughout the structure calculation procedure, the force constant for bond lengths was set to 1000 kcal mol^{-1} Å^{-2} and for bond angles and impropers (e.g., all dihedral angles, and bond angles of proline) to 500 kcal mol^{-1} rad^{-2}. An initial set of 100 random structures was generated for the uncharged FbgAα(1−16 Ser3P) peptide starting from random values for the dihedral angles ϕ, ψ, and χ and a value of 180° for the dihedral angle ω. The bound conformation of the uncharged phosphorylated peptide was then determined by incorporating the NOE distance constraints into a Powell energy minimization (EM) and simulated annealing (SA) protocol (*55*−*58*). The SA method is based on Verlet restrained molecular dynamics. For all calculations, the NOE penalty function was set to 50 kcal mol^{-1} Å^{-2}. The EM/SA protocol can be divided into five stages. First, 500 steps of Powell energy minimization were applied with a weight for the van der Waals repulsion force constant set at 0.002 and a slope for the asymptotic constant for the NOEs set at 0.1. Under these conditions, the atoms were allowed to move through each other, providing greater freedom to accommodate the initial NOE constraints. Next, conformational sampling of structures was carried out by applying 20 ps of molecular dynamics at 1000 K, with the weight for the repulsion force constant set at 0.002 and the slope for the asymptotic constant set at 0.1. Distance penalties were evaluated using a soft-well square NOE potential. In the third stage, the structures were subjected to 10 ps of molecular dynamics at 1000 K with the weight for the repulsion force constant increased to 0.1 and the slope for the asymptotic constant increased to 1.0. Under these conditions, the peptide ligand was given less freedom to sample the conformational space. For the fourth stage, the asymptotic constant remained at 1.0 and the weight for the repulsion force constant was increased to 1.0. The temperature was gradually lowered from 1000 to 100 K in 1000 steps (1 ps/step) of molecular dynamics. In the final stage, 2000 steps of Powell energy minimization were applied with a weight for the repulsion force constant of 4.0. For this stage, the soft-well square potential was replaced with a square-well potential.

Computational Docking of FbgAα(1−16 Ser3P) onto the Surface of Thrombin. Interactions between FbgAα(1−16 Ser3P) and the active-site surface of thrombin were then examined using X-PLOR 3.1 (*54*, *59*). A set of 10 best solution structures for the bound phosphopeptide was identified by the following criteria. Structures first were classified in terms of the least number of NOE violations and then in terms of the lowest backbone RMSD values. The resultant set of structures was pooled and an average structure was calculated. The 10 structures with the lowest RMSD values relative to the average were identified as the 10 best structures. All of these structures had the potential to interact with the surface of thrombin. The backbone atoms for peptide residues 7−16 were manually superimposed initially on the corresponding atoms of the X-ray structure of bovine thrombin, FpA(7−16) (*60*). To keep FbgAα(1−16 Ser3P) positioned correctly during the initial docking and energy minimization steps, a series of randomly chosen fictitious NOEs between residues 7−16 of the peptide and the enzyme were taken from the X-ray structure and incorporated into the calculations. The newly added fictitious NOEs involved distances from the peptide to the rim of the thrombin active-site surface. In addition, the critical interactions between the Arg side-chain amines of FbgAα(R16) and the γ-carboxyl of thrombin D189 were included. Without these fictitious NOEs, the peptides easily became displaced from the thrombin surface upon energy minimization.

The initial docked complexes of uncharged FbgAα(1−16 Ser3P)-thrombin were subjected to an energy minimization/simulated annealing protocol that would remove any unfavorable van der Waals interactions between the ligand and the enzyme. During all of the calculations of the

peptide−enzyme complex, the thrombin was kept fixed at its X-ray structure, and the atoms of the peptide were allowed to move and interact with potential binding surfaces on the enzyme. The peptide structures, however, were still under the control of the NMR NOE distance constraints. Only intrapeptide and peptide−thrombin interactions were calculated. The energy minimization/simulated annealing protocol was carried out by the following procedure. First, 200 steps of Powell energy minimization were applied to the complex with a weight for the repulsion force constant of 0.002 and a slope for the asymptotic constant of 0.1. Next, conformational sampling of structures was carried out by applying 6 ps of molecular dynamics at 1000 K, with the weight for the repulsion force constant set at 0.002 and the slope for the asymptotic constant set at 0.1. Distance penalties were evaluated with a soft-well square NOE potential. The structures were then subjected to 3 ps of molecular dynamics at 1000 K with the weight for the repulsion force constant increased to 0.1 and the slope for the asymptotic constant increased to 1.0. Following this, the slope for the asymptotic constant remained at 1.0 and the weight for the repulsion force constant was increased to 1.0. The temperature was gradually lowered from 300 to 100 K in 250 steps (1 ps/step) of molecular dynamics. In the final stage, 500 steps of Powell energy minimization were applied with a weight for the repulsion force constant set at 4.0. For this stage, the soft-well square potential was replaced with a square-well potential.

All fictitious NOEs except those involving FpA(R16)−thrombin(D189) were then removed, charges were added to ionizable groups, and the enzyme−peptide complex was subjected to 1500 cycles of Powell energy minimization. During this procedure, the weight for the repulsion force constant was increased to 2.0. The electrostatic interactions were calculated with a weight of 1.0. In the final stage of structure refinement, the fictitious NOEs involving FpA(R16)−thrombin(D189) were removed and a final round of 500 steps of energy minimization was applied.

RESULTS

Kinetics of Fibrinogen-like Peptides. The kinetics of hydrolysis of unphosphorylated and phosphorylated FbgAα-(1−20) were determined and compared with values observed for FbgAα(7−20) and for the entire fibrinogen Aα chain (Table 2). According to the data in Table 2, K_m for hydrolysis of peptide 1−20 is 6.5-fold higher than that for 7−20 (*61*). This difference, however, is a function of the pH value chosen for the kinetic studies. Thrombin activity toward fibrinogen exhibits a bell-shape dependence on pH with a maximum at pH 8 (*62*). As a result, the observed decrease in k_{cat}/K_m values is expected in the lower pH range. The new kinetic results reported in this paper were obtained at this lower pH to reflect the experimental conditions employed in the NMR studies more closely. The value of K_m for hydrolysis of FbgAα(1−20) was 2000 ± 350 μM, whereas K_m for FbgAα(1−20 Ser3P) was 1150 ± 210 μM. By contrast, the k_{cat} values were virtually identical for both peptides. The resulting values of k_{cat}/K_m were then (0.74 ± 0.04) × 10^{-7} vs (1.22 ± 0.12) × 10^{-7} [(NIH unit/ L)s]$^{-1}$ for the unphosphorylated and phosphorylated peptide, respectively. The substrate specificity (k_{cat}/K_m), therefore, has increased by approximately 65% upon introduction of the phosphate group. These kinetic data suggest that the phosphate group may promote further binding of FbgAα-(1−20), but the modification does not affect the catalytic constants for hydrolysis of the substrate. The differences in the values of K_m and k_{cat}/K_m observed for hydrolysis of the phosphorylated vs the unphosphorylated fibrinopeptides leads to an interest in examining the structures of both peptides bound to thrombin.

Table 2: Kinetic Constants for the Hydrolysis of Arg−Gly Bonds by Thrombin

substrate	$K_m \times 10^6$ (M)	$k_{cat} \times 10^{11}$ (M/[(NIH units/L)s])	$k_{cat}/K_m \times 10^7$ [(NIH units/L)s]$^{-1}$
human FbgAα[a]	9.5 ± 0.5	50 ± 5.0	525 ± 50
human FbgAα-P[a]	4.8 ± 0.3	32 ± 3.0	670 ± 30
Ac−Fbg(7−20)-Am[b]	310 ± 99	31 ± 7.0	10 ± 5
NH-Fbg(1−20)-H[c,d]	2000 ± 350	15 ± 2.5	0.74 ± 0.04
NH-Fbg(1−20P)-H[d]	1150 ± 210	14 ± 2.2	1.22 ± 0.12

[a] These lines pertain to the chains in the intact fibrinogen molecule. Values for human FbgAα and FbgAα-P were determined by Hanna et al. (*38*) at pH 8.0, 25 °C. [b] Ac−FbgAα(7−20)-Am corresponds to Ac(DFLAEGGGVRGPRV)amide. Values were determined by Marsh et al. (*61*) at pH 8.0, 25 °C [c] NH−FbgAα(1−20)-H corresponds to NH_3^+(ADSGEGDFLAEGGGVRGPRV)COOH. Serine at position 3 is phosphorylated in the next peptide. pH 6.3, 25 °C. [d] Kinetic constants for hydrolysis of these peptides were determined as described under Experimental Procedures. The results shown here represent averages of at least three independent experiments. The kinetic values reported for Fbg(1−20) and Fbg(1−20P) were calculated by linear least-squares analysis. Similar ratios for the Michaelis−Menten kinetic constants for phosphorylated vs unphosphorylated peptide were found using nonlinear regression.

1D Proton Line Broadening Studies. One-dimensional proton NMR spectra were collected for the free peptides and for the thrombin−FbgAα(1−20Ser3P), thrombin−FbgAα-(1−20), and thrombin−FbgAα(1−16Ser3P) complexes. FbgAα(1−20) and (1−20Ser3P) were at least 80% hydrolyzed at the Arg16−Gly17 cleavage site by the time that the first NMR measurements were taken. Spectra were monitored until a consistent pattern of peaks for the hydrolyzed peptide was obtained. The chemical shift patterns of the hydrolyzed peptides were in agreement with those reported by Ni et al. (*37*, *47*) for FbgAα(1−16), also known as FpA. Upon hydrolysis by thrombin, Arg16 becomes the C-terminal amino acid and the NH chemical shift of this residue moves upfield from 8.50 to 8.05 ppm. This chemical shift change occurs for both the phosphorylated and unphosphorylated fibrinopeptides. In addition, proton peaks corresponding to ^{17}GPRV^{20} are no longer visible. Ni et al. (*37*) had shown earlier that the G17−V20 sequence binds very weakly to thrombin. The present study indicates that this sequence does not interfere with observations of the bound structure of FbgAα(1−16).

The amide proton regions of the NMR spectra of FbgAα-(1−20 Ser3P) and the thrombin−FbgAα(1−20 Ser3P) complex are highlighted in Figure 1. In the presence of the enzyme, the NH peaks of the individual amino acid residues were examined for changes in line width and line character. The amide proton peaks for the N-terminal amino acids D2, S3, G4, and E5 each exhibited broadening relative to those of the free peptide. Line broadening was also observed for the amide protons of amino acids 7−16. As is often the case with N-terminal amino acids, the amide proton of A1

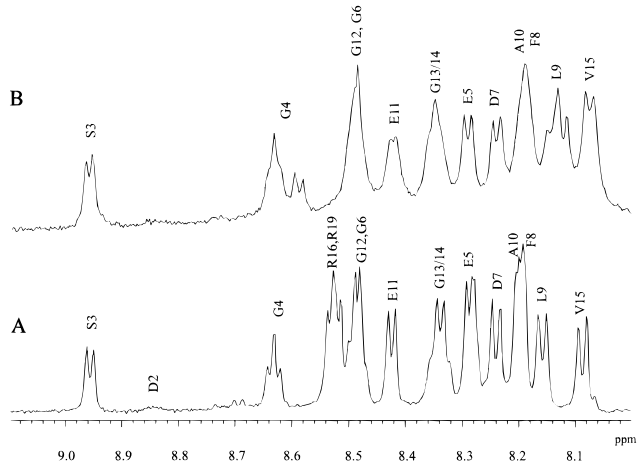

FIGURE 1: Effect of native bovine thrombin on the 1D amide proton NMR spectrum of FbgAα(1−20 Ser3P). (A) Spectrum for 2 mM FbgAα(1−20 Ser3P) in 25 mM H_3PO_4, pH 5.6, 150 mM NaCl, and 0.2 mM EDTA. (B) Spectrum for 2 mM FbgAα(1−20 Ser3P) and 160 μM bovine thrombin in the same buffer. All spectra were referenced against HOD 4.80 ppm.

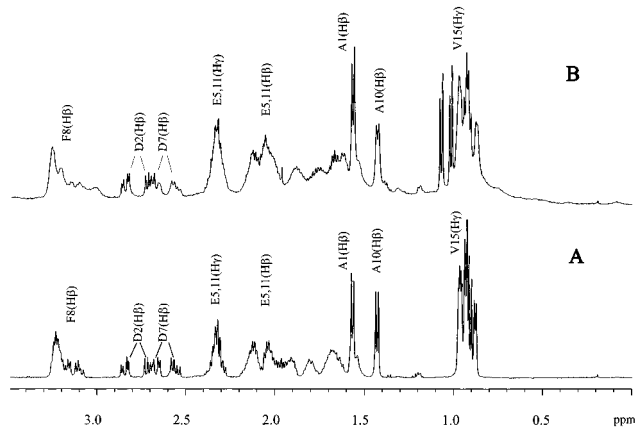

FIGURE 2: Effect of native bovine thrombin on the 1D aliphatic proton NMR Spectrum of FbgAα(1−20 Ser3P). Same conditions were used for spectra A and B as in Figure 1.

was not observed for either the phosphorylated or unphosphorylated peptide. Ni et al. (*47*) reported that the NH proton of D2 is relatively mobile and, therefore, difficult to observe. The spectra shown in Figure 1 are in agreement with this proposal. To evaluate the interaction of D2 with thrombin better, the C$^{\beta}$H region was examined. As seen in Figure 2, introduction of thrombin causes the peaks from the C$^{\beta}$H protons of D2 to broaden slightly. In this figure, additional characteristic broadening effects are seen for the side-chain protons of D7, F8, A10, E11, and V15. The same type of line broadening was also observed for FbgAα(1−16 Ser3P) in the presence of thrombin. By contrast, for the unphosphorylated peptide, line broadening begins only at G6 (data not shown). This absence of line broadening for the N-terminal amino acids supports previous conclusions that FbgAα(1−5), in the unphosphorylated state, does not come in contact with the thrombin surface. The new line broadening effects observed for the phosphorylated peptide suggest that the presence of the phosphoserine helps promote additional interactions between the N-terminal portion of FbgAα and the thrombin surface.

NMR 2D-TRNOESY. Two-dimensional TR-NOESY experiments were conducted for native thrombin in the presence of a 10−15-fold excess of phosphorylated or unphosphorylated fibrinogen Aα-like peptides. Similar results were obtained for both the 1−20 and 1−16 peptides. Once again, this information indicates that, when thrombin hydrolyzes the peptides at the Arg16−Gly17 bond to produce fibrinopeptide A (FbgAα1−16), the released product G17−V20 does not bind significantly to thrombin, nor does it interfere with the bound structure of 1−16. Work was continued with the whole peptide to verify that the thrombin samples that were buffer-exchanged for NMR studies were still active toward hydrolyzing substrates.

As mentioned previously, fast exchange of peptide on/off the surface of the enzyme is desired for transferred NOESY experiments. Under slow exchange, separate peptide signals from both free and bound states may occur instead of the single peak reflecting contributions from both states. Two-dimensional transferred NOESY spectra for the thrombin−fibrinopeptide complexes analyzed in this study were examined to see if any peaks exhibiting slow chemical exchange characteristics were present.

Spectra in the chemical shift range of 5.5−9.0 ppm were compared to those reported by Ni et al. (*63*) for wild-type fibrinopeptide A [FpA(7−16) or FbgAα(7−16)] and for FpA(7−16) containing a Pro substituted for Val15 (P15FpA). In the presence of thrombin, the P15FpA spectra contained several cross-peaks in this chemical shift range that suggested the presence of slow exchange between the free and bound states. By contrast, the spectra for wild-type FpA(7−16)−thrombin contained only a very weak cross-peak representing the free/bound states of F8 C$^{\epsilon}$H. The weak nature of this cross-peak suggests that only a very minor population of the peptide exhibits slow chemical exchange characteristics. The value of k_{off} for P15FpA was estimated to be 100 s^{-1} as opposed to $k_{off} > 300$ s^{-1} for wild-type FpA(7−16).

In the presence of thrombin, the 2D TR-NOESY spectra of the peptides FbgAα(1−20), (1−20Ser3P), and (1−16Ser3P) also all contained only a very weak cross-peak between free/bound F8 C$^{\epsilon}$H (F8 H$^{\epsilon f}$/H$^{\epsilon b}$). No other cross-peaks suggesting slow chemical exchange were present. A spectrum for the thrombin−FbgAα(1−20 Ser3P) complex is shown in Figure 3 with the F8 H$^{\epsilon f}$/H$^{\epsilon b}$ cross-peak highlighted. On the basis of a comparison with the spectrum reported by Ni et al. (*63*) for the FpA−thrombin complex, we therefore conclude that the phosphorylated and unphosphorylated peptides examined in this study undergo the same fast exchange on/off the surface of thrombin with a $k_{off} > 300$ s^{-1}.

The 2D transferred NOESY spectra of phosphorylated and unphosphorylated peptide bound to bovine thrombin were examined for the characteristic NOE effects reported by Ni et al. (*64*). Through-space interactions observed for the phosphorylated peptide are summarized in Table 3. The unique hydrophobic cluster, involving long-range interactions between F8, L9, V15, and G13/14, recorded previously (*64*) for thrombin−FbgAα(7−16), was also present for FbgAα-(1−20), FbgAα(1−20 Ser3P), and FbgAα(1−16 Ser3P) in the presence of native bovine thrombin. Distinctive NOEs observed include L9 C$^{\delta}$H− F8 (C$^{\delta}$H, C$^{\epsilon}$H); L9 C$^{\gamma}$H−F8 (C$^{\delta}$H, C$^{\epsilon}$H); V15 C$^{\gamma}$H−F8 (C$^{\delta}$H, C$^{\epsilon}$H); F8 C$^{\beta}$H−F8 C$^{\delta}$H; V15 C$^{\alpha}$H− F8 (C$^{\epsilon}$H, C$^{\delta}$H); G13/G14 C$^{\alpha}$H−F8 (C$^{\delta}$H, C$^{\epsilon}$H, C$^{\zeta}$H); L9 C$^{\alpha}$H− F8 (C$^{\epsilon}$H, C$^{\delta}$H); and F8 C$^{\alpha}$H− F8 (C$^{\epsilon}$H, C$^{\delta}$H). From these results, we may conclude that the

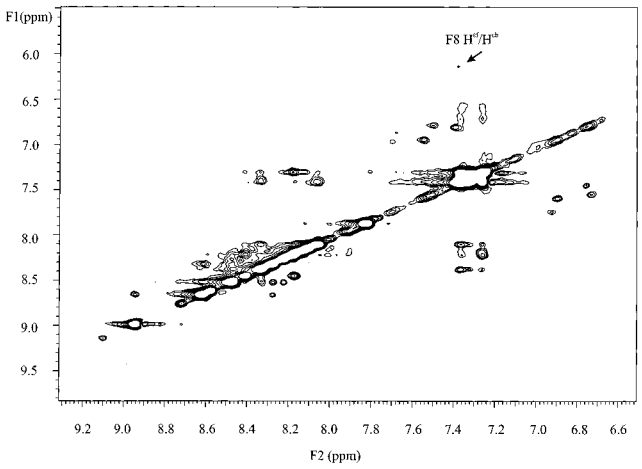

FIGURE 3: Examination of 2D transferred NOESY spectrum of bound fibrinopeptide A(Ser3P) for the presence of slow chemical exchange peaks. Experimental conditions for this spectrum are as follows: 1.6 mM FbgAα(1−20 Ser3P), 160 μM bovine thrombin, 25 mM H_3PO_4, 150 mM NaCl, and 0.2 mM EDTA, 500 MHz, 32 transients, 512 FIDs, delay time 1.5 s, mixing time 400 ms, 25 °C. All spectra were referenced against HOD 4.80 ppm.

characteristic hydrophobic peptide cluster is maintained in the presence of phosphoserine. The NOEs observed by Zheng et al. (*65*) involving the ring protons of F8 ($C^{\delta,\epsilon,\zeta}H$) and the NH of V15 and between F8 ($C^{\delta,\zeta,\epsilon}H$) and the NH of G13/14 were also present. In addition, characteristic NOEs for D7 $C^{\beta}H$−A10 $C^{\beta}H$, D7 NH−A10 $C^{\beta}H$, and D7 NH−E11 $C^{\gamma}H$ were all present, providing further support for a distinctive turn structure of the bound fibrinopeptides.

In addition to the similarities in observed NOE cross-peak patterns, there was a distinct set of differences. The newly observed through-space interactions are described as follows:

NOE Map of $C^{\alpha}H$−NH Connectivities and NH−$C^{\beta}H$. As can be seen in Figure 4, there are differences in the connectivity pattern between the phosphorylated and unphosphorylated peptides in the presence of thrombin. In the unphosphorylated state, the connectivities can be drawn from D2 through G4 and then from E5 through to R16. Furthermore, a NH−$C^{\beta}H$ cross-peak is not observed for S3. When S3 is phosphorylated, the NH chemical shift for this amino acid moves downfield from 8.65 to 8.93 ppm and the $C^{\beta}H$ moves downfield from 3.96 to 4.15. Also in response to this modification, a cross-peak representing the S3 NH−$C^{\beta}H$ interaction appears. As is observed with the free peptide at pH 5.6, the β/β' protons are degenerate and thus are described by a single peak. When the pH of the free peptide is lowered from 5.6 to 4.1, the β/β' resonances become distinguishable and appear as a doublet. Thrombin begins to precipitate out of solution at pH values less than 5.3 and thus transferred NOESY experiments on the enzyme−peptide complexes could not be carried out at pH 4.1. Phosphorylation at S3 also affected the NH chemical shift position of E5, causing it to move upfield from 8.33 to 8.26 ppm. With this modification by phosphorylation, an NOE for G4−E5 ($C^{\alpha}H$−NH) appeared that could not be observed for the enzyme−unphosphorylated peptide complex. The fact that the NH proton for E5 did not exhibit a downfield shift in response to the phosphorylated serine suggests that the NH of E5 may not participate in hydrogen-bond interactions with the phosphate group. The changes in the NOE cross-peak pattern observed for the phosphorylated peptide now allow $C^{\alpha}H$−NH connectivities to be drawn from D2 all the way through to R16.

Amide−Amide Region. Interactions in this region of the spectrum could best be observed at 15 °C (Figure 5). For the unphosphorylated peptide, NH−NH NOEs are observed for G4−E5, E11−G12, G12−G13, A10−E11, and G13/14−V15. The NOES from A10 through V15 are in agreement with those reported by Ni et al. (*64*). The introduction of the phosphorylated serine leads to the observation of an NOE for S3−G4 NH−NH.

^{31}P NMR Studies. A series of one-dimensional ^{31}P NMR spectra were collected for FbgAα(1−20 Ser3P), FbgAα(1−20 Ser3P)−thrombin, and FbgAα(1−16 Ser3P)−thrombin. The ratio of thrombin to peptide varied from 1:10 to 1:15. A single peak for phosphorylated serine was monitored for changes in line width and chemical shift. As seen in Figure 6, the chemical shift of the Ser3P moved downfield from 1.47 to 1.62 ppm in response to changes in environment and/or structure occurring upon formation of a thrombin−FbgAα-(1−20 Ser3P) complex. Furthermore, the ^{31}P NMR line width doubled, providing additional evidence that Ser3P interacts directly with the surface of the thrombin.

To obtain an estimate of the pK_a value of the Ser3P, the chemical shift position of the ^{31}P NMR peak was monitored as a function of pH for FbgAα(1−20 Ser3P) (pH 2.27−7.4). As the pH increased, the chemical shift moved further downfield in response to changes in the ionization state of the phosphate, and a typical sigmoidal titration pattern was produced. The pK_a for the second ionization state of the phosphate was determined to be in the range of 5.5−6.5.

Experiments were then carried out to determine whether the phosphorylated fibrinopeptide could still interact with thrombin if the active site was blocked. Thrombin was incubated with the small synthetic inhibitor PPACK, which bound covalently to the enzyme. The active site of the enzyme was verified to be blocked when the complex could no longer hydrolyze S2238. Further proof that the catalytic site could not be accessed by fibrinopeptides was provided from the 1D and 2D spectra of the PPACK-thrombin−FbgAα(1−20 Ser3P) complex. The proton chemical shifts for the 1D spectra and the $C^{\alpha}H$−NH connectivities for the 2D transferred NOESY spectra were the same as those of the intact 20-residue peptide free in solution. These observations provide additional support that the active site of thrombin could no longer bind and hydrolyze its substrates. Furthermore, the peptide in the presence of PPACK-thrombin could not form the distinct hydrophobic binding cluster involving F8, L9, and V15. The ^{31}P NMR spectra of PPACK-thrombin−FbgAα(1−20 Ser3P), however, revealed that the peak for Ser3P could still become broadened relative to that of the free peptide. These results suggest that the phosphoserine can interact with thrombin even though the active site is blocked. The characteristic hydrophobic peptide cluster is not required to help position the Ser3P toward its own specific thrombin binding site.

Calculation of the Bound Structure of FbgAα(1−16 Ser3P). In the spectra of the free and bound fibrinopeptides, the NH and $C^{\alpha}H$ chemical shifts for G13 and G14 are superimposed. Ni et al. (*64*) demonstrated that cross-peaks between F8 and G14 ($C^{\alpha}H$) could still be observed when a peptide containing deuterated C^{α} G13 was examined. From these results, it was concluded that F8 is closer to G14 than

Table 3: ^{1}H Transferred NOESY Connectivities for Bound Structure of FpA(Ser3P)[a]

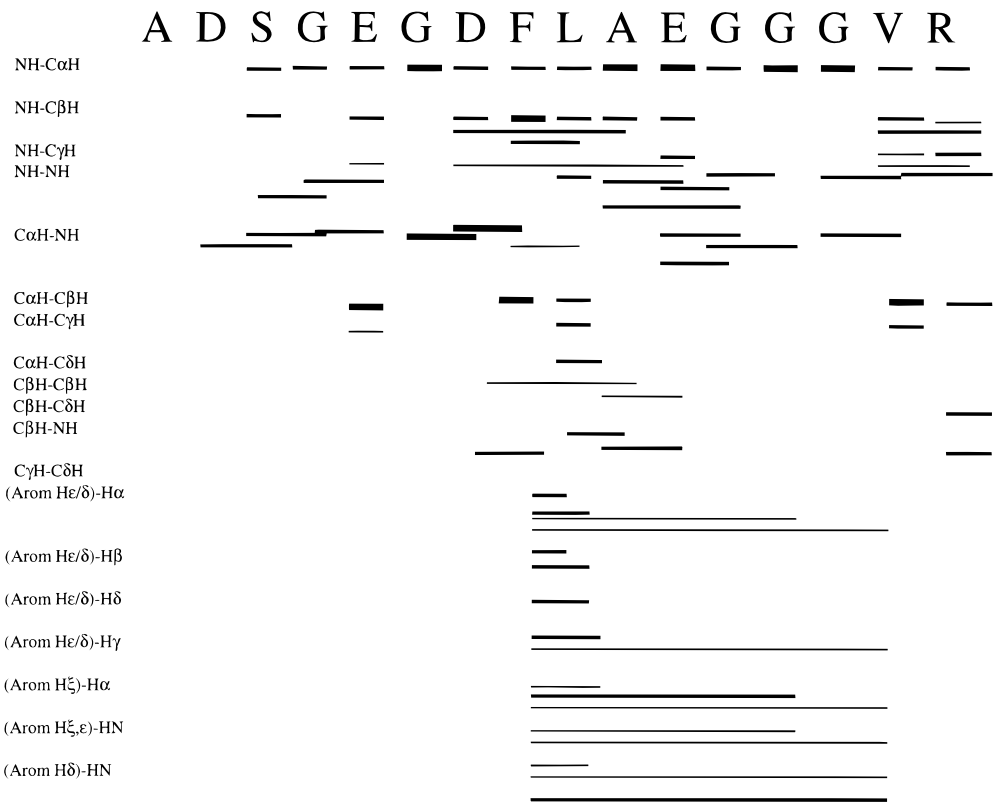

[a] NOE distance constraints were derived from transferred NOESY experiments conducted at 250 ms. Cross-peaks were classified as strong [1.8−(2.6 ± 0.25) Å], medium [1.8−(3.3 ± 0.25) Å], and weak [1.8−(4.8 ± 0.25) Å] on the basis of the number of contour levels visible. The thicker the line, the shorter the through-space distance.

G13. This conclusion was verified (*63*) by experiments involving P15FpA in which the chemical shifts of G13 and G14 were differentiable. As a result of these findings, ambiguous G13/G14 cross-peaks recorded in the current study were first assigned to G14, and structure calculations were carried out using both the DIANA program (*66*−*68*) (data not shown) and the XPLOR package. The characteristic helical turn found for residues 7−16 could be produced but the subsequent structures were too compact (data not shown). This problem continued even after taking into account the possibility of spin diffusion problems involving the aromatic protons of F8. The results therefore suggest that interactions involving G13 might also contribute to the observed NOEs.

The NOE constraint file generated for bound P15FpA (*63*) was then compared with that from the FbgAα(1−20 Ser3P) project. NOE constraints involving G13 that were observed for bound P15FpA were then added into the NOE constraint file for bound FbgAα(1−16 Ser3P). New NOEs included in the calculations were 8Phe $C^{\zeta,\delta,\epsilon}$H−13Gly C^{α}H and 8Phe C^{δ}H−13Gly HN. These additional NOEs allowed the bound conformation of residues 7−16 to relax, resulting in structures that were in greater agreement with those found in previously published NMR and X-ray studies.

An ensemble of best structures for bound FbgAα(1−16 Ser3P) derived from the XPLOR 3.1 package is shown in Figure 7A. Calculations were carried out for the thrombin-bound peptide, but in the absence of the enzyme, and with an uncharged phosphate group on serine 3. Amino acids 7−16 of such a thrombin-bound peptide adopt a unique helical-turn conformation. F8 is directed toward the peptide cleavage site and, together with L9, G13/14, and V15, forms a hydrophobic cluster. The side chain for the C-terminal R16 can adopt a number of different orientations because the enzyme active-site cavity is not present in the calculations to constrain the structure of this side chain. As can be seen in Figure 7A, there is also much variability in the conformation of the N-terminal segment of the peptide involving amino acids 1−5. This segment of the peptide can have both extended and turnlike characteristics. The structures obtained for FbgAα(1−16 Ser3P) satisfied the NOE distance constraints used for the calculations with no distance violation greater than 0.3 Å.

Backbone and heavy atom RMS deviations were then calculated relative to a low energy average structure. For amino acids FbgAα(1−16), the RMSD values were 2.06 ± 0.45 Å for the backbone atoms and 2.74 ± 0.42 Å for all heavy atoms. For amino acids FbgAα(1−6), the RMSD values were 1.58 ± 0.31 Å for the backbone atoms and 2.92 ± 0.38 Å for all heavy atoms. For amino acids FbgAα(7−16), the RMSD values were 0.34 ± 0.24 Å for the backbone atoms and 0.64 ± 0.25 Å for all heavy atoms. RMS deviations were also calculated for amino acids 7−16 relative to the X-ray structure of bound 7−16 (*60*). The values were 1.25 ± 0.12 Å for the backbone atoms and 2.11 ± 0.19 Å for all heavy atoms. A summary of the XPLOR energies, NOE violations, and RMSD values can be found in Table 4. For comparison, RMSD values were also calculated for the DIANA-derived structures relative to the X-ray structure of 7−16 (*60*). The RMSD values for amino acids 7−16

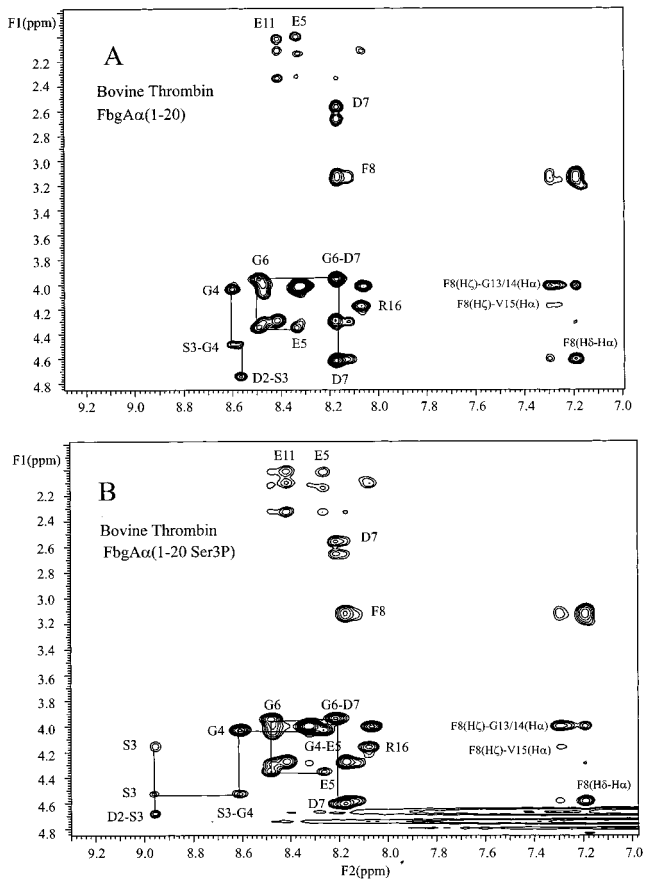

FIGURE 4: Highlighted regions of 2D transferred NOESY spectra of fibrinopeptide A and fibrinopeptide A(Ser3P) bound to native bovine thrombin. (A) Spectrum for 1.4 mM FbgAα(1−20) and 137 μM bovine thrombin in 25 mM H_3PO_4, pH 5.6, 150 mM NaCl, and 0.2 mM EDTA. (B) Spectrum for 1.6 mM FbgAα(1−20 Ser3P) and 160 μM bovine thrombin in the same buffer. NMR conditions for both spectra were 500 MHz, 32 transients, delay time of 1.5 s, 512 FIDs, τ_{mix} = 250 ms, 15 °C. All spectra were referenced against HOD 4.80 ppm.

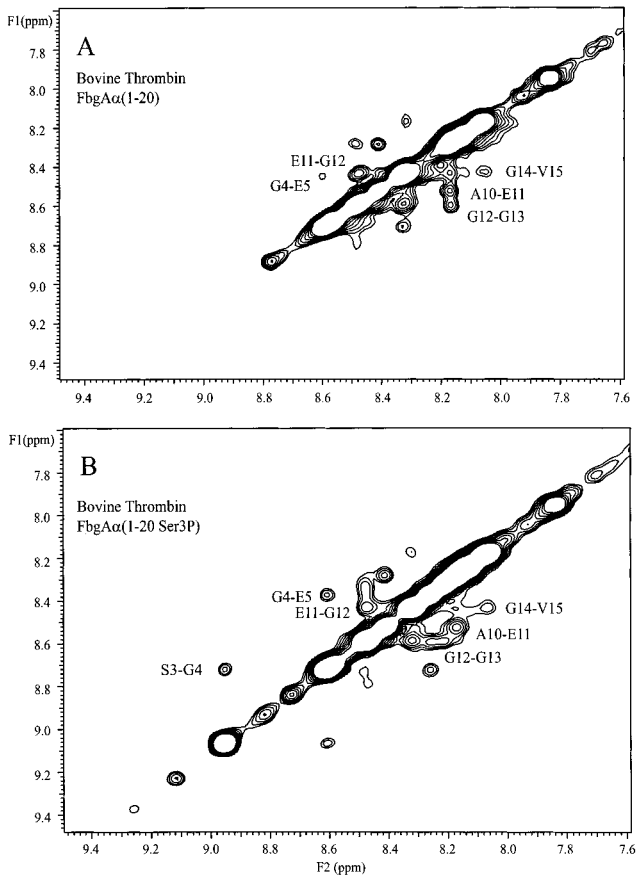

FIGURE 5: Amide−amide region of 2D transferred NOESY spectra of fibrinopeptide A and fibrinopeptide A(Ser3P) bound to native bovine thrombin. Experimental conditions are the same as those in Figure 4. The spectra in both Figures 4 and 5 pertain to 15 °C.

were 1.36 ± 0.04 Å for backbone atoms and 3.67 ± 0.15 Å for all heavy atoms. When considering these values, it should be noted that the DIANA structures were not subjected to the more rigorous refinement process applied to the XPLOR structures.

Computational docking of the FbgAα(1−16 Ser3P) solution structures onto thrombin would provide a means for assessing whether a more defined conformation for amino acids 1−5 appears upon interaction with the enzyme surface. The resultant complexes could also be examined for possible binding sites for Ser3P. The XPLOR 3.1 package was used for the docking procedure, and the XPLOR 3.1-generated solution structures were chosen over the DIANA-generated structures for greater ease in incorporating the peptide into the calculations. Fictitious NOEs involving distances between the peptide and the rim of the thrombin active site and between the arginine side chains of FbgAα(R16) and the γ-carbonyl of thrombin D189 were needed to keep the peptide positioned correctly during the initial docking and energy minimization steps. Later in the procedure all fictitious NOEs except those involving FbgAα(R16)−thrombin(D189) were removed and charges were added to the ionizable groups. For the last step of structure refinement, even the fictitious NOEs involving FbgAα(R16)−thrombin(D189) were also deleted from the calculations.

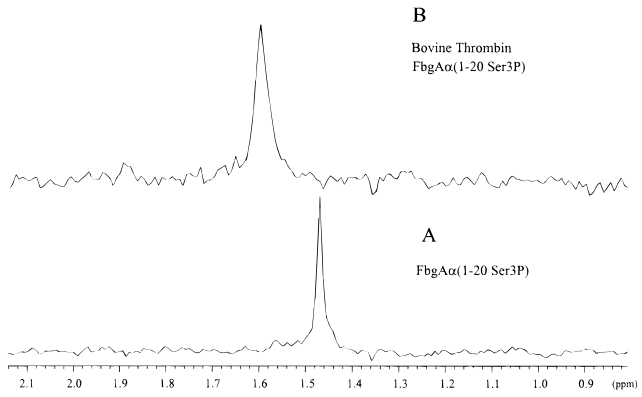

FIGURE 6: Effect of native bovine thrombin on the ^{31}P NMR spectrum of FbgAα(1−20 Ser3P). (A) Spectrum for 2 mM FbgAα-(1−20 Ser3P) in 25 mM H_3PO_4, pH 5.6, 150 mM NaCl, and 0.2 mM EDTA. (B) Spectrum for 2 mM FbgAα(1−20 Ser3P) and 160 μM bovine thrombin in the same buffer. Spectra were referenced against H_3PO_4, 0.0 ppm.

Even though these final NOEs involving FbgAα(R16) were removed, the side chain for this amino acid still remained in the active-site pocket and continued to interact with thrombin D189.

As can be seen in Figure 7B, the presence of enzyme has reduced the variability in conformation for FbgAα amino acids 1−5. This N-terminal segment is still considered flexible but can now be resolved into a more defined cluster. The RMS deviations for the docked peptides relative to an average structure were 1.11 ± 0.14 Å (backbone atoms) and

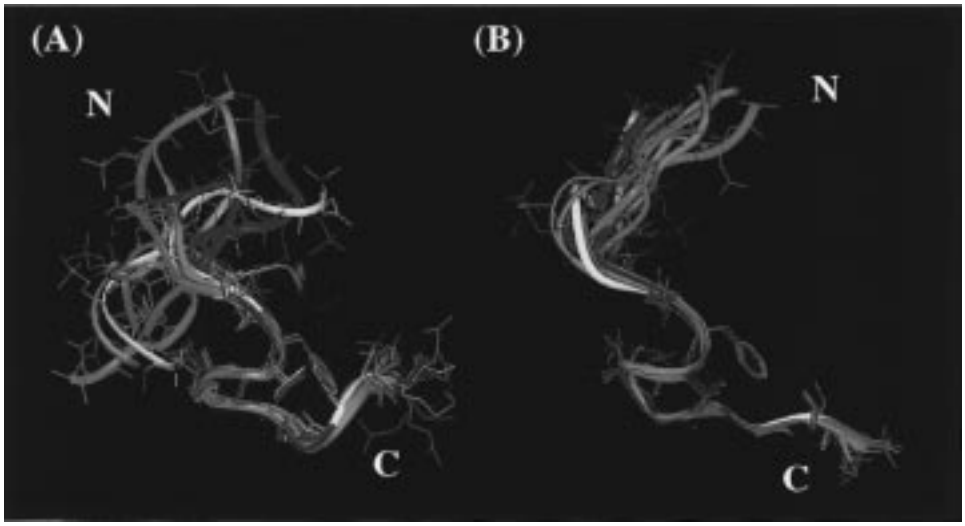

FIGURE 7: Ensemble of structures for bound peptide FbgAα(1−16 Ser3P). The XPLOR 3.1 program was used to obtain a set of structures for the bound peptide. Upper and lower distance constraint files were generated by evaluating the intensities of NOE cross-peaks observed at a mixing time of 250 ms. The N-terminus of the peptide is NH_3^+ and the C-terminus is COO^-. (A) and (B) pertain to structure calculations in the absence and presence, respectively, of enzyme.

Table 4: Refinement Statistics for the FgbAα(1−16 SerP) Bound to Bovine Thrombin

	bound FgbAα(1−16 SerP)	
	before docking	after docking
X-PLOR Energies (kcal mol^{-1})		
E_{tot}	36.78 ± 6.12	−113.64 ± 16.52
E_{VDW}	−3.05 ± 4.28	−72.44 ± 14.20
E_{NOE}	9.91 ± 3.05	10.55 ± 4.90
E_{elec}	*a*	−125.64 ± 20.09
E_{bond}	5.07 ± 0.65	20.81 ± 4.92
E_{angle}	21.67 ± 1.72	46.92 ± 10.21
E_{impr}	3.18 ± 0.83	6.17 ± 1.06
NOE violations		
>0.3 Å	0	0
>0.1 Å	6	10

	Cartesian Coordinate RMSD[b] (Å)			
	before docking		after docking	
structure	backbone	all heavy atoms	backbone	all heavy atoms
1−16	2.06 ± 0.45	2.74 ± 0.42	1.11 ± 0.14	1.90 ± 0.17
1−6	1.58 ± 0.31	2.92 ± 0.38	1.17 ± 0.15	2.62 ± 0.26
7−16	0.34 ± 0.24	0.64 ± 0.25	0.23 ± 0.12	0.58 ± 0.13
7−16 vs X-ray (7−16)	1.25 ± 0.12	2.11 ± 0.19	0.53 ± 0.06	1.21 ± 0.06

[a] Electrostatics were not included in these initial calculations in order to focus on elimination of steric overlaps and to provide greater weight to the NOEs. [b] Average of RMSDs between each structure and the average structure, or the X-ray structure, respectively.

1.90 ± 0.17 Å (heavy atoms) for FbgAα(1−16), 1.17 ± 0.15 Å (backbone atoms) and 2.62 ± 0.26 Å (heavy atoms) for FbgAα(1−6), and 0.23 ± 0.12 Å (backbone atoms) and 0.58 ± 0.13 Å (heavy atoms) for FbgAα(7−16). RMSD values were also calculated for amino acids 7−16 of the docked peptides relative to the X-ray structure (*60*) of bound 7−16. The values were 0.53 ± 0.06 Å for the backbone atoms and 1.21 ± 0.06 Å for the heavy atoms. A summary of the refinement statistics can be found in Table 4.

DISCUSSION

Previous NMR studies carried out by Ni et al. (*37*) and now confirmed here indicate that the first five amino acids of the FbgAα chain, ADSGE, do not interact with the surface of thrombin. Twenty-five to 30% of human fibrinogen Aα, however, becomes phosphorylated at the serine 3 position, and the structural reason for this modification is not understood. For this study, the effect of phosphorylation on binding of both fibrinogen Aα(1−20) and its hydrolysis product fibrinopeptide A [or FbgAα(1−16)] to thrombin were examined by kinetic and nuclear magnetic resonance methods. The experimental results suggest that introduction of the phosphoserine promotes new interactions between FbgAα(1−5) and the thrombin molecular surface.

Effect of Phosphorylation on the Kinetics of Hydrolysis of FbgAα(1−20) by Thrombin. Kinetic studies indicate that phosphorylation leads to an approximately 65% increase in the value of k_{cat}/K_m for hydrolysis of FbgAα(1−20). The increase in k_{cat}/K_m reflects a decrease in the value of K_m and little change in the value of k_{cat}. These results suggest that phosphorylation plays a role in increasing the specificity of thrombin for FbgAα-like peptides but has little effect on the

turnover rate. The relative changes that occur between the kinetic parameters of FbgAα(1−20) and FbgAα(1−20 Ser3P) at pH 6.3 are similar to those that were reported by Hanna et al. (*38*) at pH 8 for the entire FbgAα chain in the phosphorylated vs unphosphorylated state. Experiments at pH 8 would have increased the overall ability of thrombin to hydrolyze the peptides. This improvement is evident in the kinetic parameters determined for FbgAα(7−20) at pH 8 by Marsh et al. (*61*). Aside from the differences in pH, the complete Aα chain beyond residue 20 may be involved in interactions with thrombin or with other fibrinogen chains that cannot be taken advantage of by the smaller FbgAα-like peptides. The phosphate group on the serine could participate in additional stabilizing interactions with a portion of the Aα chain quite distant from amino acids 1−20 or could participate in intermolecular interactions between neighboring Aα chains of the fibrinogen dimer $(A\alpha B\beta\gamma)_2$. The shorter peptides described in this work were designed instead to explore ligand interactions within the vicinity of the thrombin active site by NMR methodologies. The lower pH of 6.3 was chosen instead for the kinetic experiments to match the conditions used in the structural studies and to guarantee that no phosphate could be removed from the peptide. The at-most 2-fold decrease in K_m observed, even for the complete FbgAα (Ser3P) chain at pH 8, suggests that this modification alone does not play a major role in enhancing the catalytic efficiency of the thrombin. The modification instead is likely to be one contributing element in the carefully regulated system of thrombin activity and inhibition.

NMR Studies of the Bound Structures of Phosphorylated vs Unphosphorylated FbgAα(1−20). One-dimensional NMR studies provide strong evidence that phosphorylation at serine 3 promotes binding of amino acids 1−5 to the thrombin surface. The proton spectra showed distinct protein-induced line broadening effects for the NH protons of D2, S3, G4, and E5, and one-dimensional ^{31}P spectra exhibited line broadening and line shape changes for the bound Ser3P. Two-dimensional transferred NOESY studies revealed through-space interactions involving the N-terminal portion of FbgAα that were not observed with the free peptide or with the bound unphosphorylated peptide. Phosphorylation of FbgAα-(1−20) caused a downfield chemical shift change for the $C^{\beta}H$ of Ser3 and an upfield chemical shift change for the NH of Glu 5. These changes eliminated potential overlaps between the chemical shifts of Gly4 $C^{\alpha}H$ and Ser3 $C^{\beta}H$ and between Glu5 NH and Gly13/14 NH. In addition, phosphorylation caused a significant downfield shift of the Ser3 NH relative to the Gly4 NH. As a result of these different changes in chemical shift, any NOE cross-peaks involving through-space interactions of S3−G4 and G4−E5 could be observed more easily. The fact that FbgAα amino acids 2−5 exhibited line broadening only with the phosphorylated peptide suggests that the newly observed NOEs indeed represent structural information about the entire phosphorylated peptide bound to thrombin.

A series of structures generated for the bound conformation of FbgAα(1−16 Ser3P) are shown in Figure 7. The 7−16 portion of FbgAα(1−16 Ser3P) results in structures that are in good agreement with previously published NMR (*63*, *64*) and X-ray work (*60*). By contrast, there is variability in the orientation of the N-terminal segment of the peptide involving amino acids 1−5. This segment is in a mostly extended structure but it can have turnlike tendencies. The N-terminal portion of FbgAα(1−16 Ser3P) may have been designed to be flexible, thus allowing it to exist in multiple conformations depending upon the enzyme environment encountered. ^{31}P NMR experiments with PPACK-thrombin revealed that part of FbgAα(1−20 Ser3P) could bind to thrombin even though the active site was blocked. Previous work has already suggested that FbgAα(1−6) is intrinsically more flexible than FbgAα(7−16) on the basis of the NH proton exchange properties of the free peptide and on an evaluation of the peptide chemical shift values relative to free amino acids (*47*). The individual amino acid residues of the N-terminal segment of FbgAα, including serine 3 found in humans, are highly variable between species and are often without strict preference for amino acid type. By contrast, amino acids within the segment 7−16 are quite conserved and form distinct structural features. Therefore, the variability of amino acids 1−5 may provide further support for the flexibility hypothesis (*31*, *32*).

Evaluation of the Role of pH in Binding of FbgAα(1−20 Ser3P) to Thrombin. Several convincing pieces of evidence have demonstrated that the phosphate at the Ser3 position promotes further interactions between the N-terminal portion of the fibrinogen Aα chain and thrombin. To obtain a better understanding of how this structural effect is accomplished, the biochemical characteristics of the modified serine must be examined. Previously published work on the statistical coil peptide GGS(P)A and on phosphorylated β-casein (*69*, *70*) indicates that the pK_a values for the phosphate of a phosphoserine are approximately 3 and 6. The pH titration of FbgAα(1−20 Ser3P) reported here provided a similar estimate for the pK_a of the second ionization state.

Depending on the pH values used, Ser3 phosphate may exhibit monoanionic and/or dianionic character. In the dianionic state, the amino acid displays a unique double charge character not observed in naturally occurring amino acids (*71*). The system in the NMR experiments at pH 5.6 is likely to contain some monoanionic Ser3 phosphate species, whereas that in the kinetic studies at pH 6.3 is likely to contain an excess of dianionic species. Several of the new NOEs observed for phosphorylated FbgAα(1−20) bound to thrombin involved exchangeable protons, thereby limiting the ability to examine these interactions at physiological pH 7.4. As mentioned previously, kinetic studies were carried out at lower than physiological pH in order to mimic the NMR conditions but still allow for reasonable hydrolysis of peptide substrates.

Work by Mavri and Vogel (*72*), however, indicates that the characteristic features of ion pair formation between phosphoserines and Lys or Arg side chains can occur under both mono- and dianionic conditions. Interactions between phosphoserine and Lys/Arg side chains were modeled by using methyl phosphate and methylamine/methylguanidinium, respectively. Ab initio and semiempirical methods were then used to calculate interaction energies and distances for the complexes involving the basic side-chain analogues and the phosphate compounds. Energetically stable ion pairs could be formed with both mono- and dianionic phosphate species. From these observations, Mavri and Vogel predicted that the reductions in intracellular pH recorded in cancer cells, anoxic cells, and contracting muscles would not lead

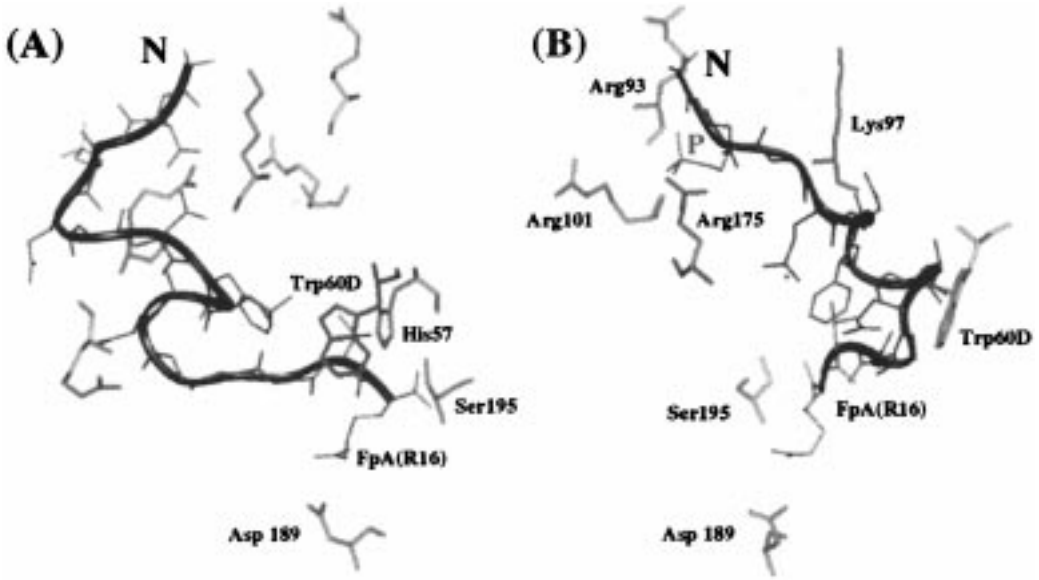

FIGURE 8: Docking of the NMR structure of bound FPA(1−16 Ser3P) onto the X-ray structure of native bovine thrombin using XPLOR 3.1. *(*Green) A representative low-energy docked structure for FpA(Ser3P). (Blue) Highlighted amino acids of thrombin from the X-ray structure of Martin et al. (*60*). The highlighted letter P in red represents the phosphate group on Ser3. N refers to the N-terminus of the fibrinopeptide. Panel A shows the docked peptide with respect to the active site of thrombin; panel B shows another view of the docked complex, rotated to emphasize the interactions between Ser3P and residues in the heparin binding site.

to disruption of ion pairs involving monoanionic phosphoamino acids. This same hypothesis can be applied to the interactions observed between the phosphopeptide and thrombin; i.e., peptides containing monoanionic serine species are predicted to be able to form stabilizing ion-pair interactions involving thrombin.

Mathur et al. (*62*) have developed a model that describes the pH dependence of the thrombin−fibrinogen interaction and the effects on the transition to the fast form of the enzyme. Fibrinogen exhibits a greater affinity for the fast (Na^+-bound) than the slow (Na^+-free) form of thrombin. Linkage thermodynamic principles, therefore, suggest that fibrinogen binding participates in the transition from the slow to the fast form of the enzyme. An examination of the effect of pH on the K_d of the thrombin−fibrinogen complex reveals that fibrinogen binding to thrombin is linked to proton release below pH 8 and to proton uptake above pH 8. This phenomenon is similar to proton release and uptake in the association of fibrin monomer (*73*, *74*). The shape and slopes of the pH dependence curve for the fibrinogen−thrombin complex suggest that the system is controlled by two ionizable amino acids from thrombin, His57 and Ile16 (chymotrypsinogen numbering is employed for all thrombin residues mentioned). For optimal substrate binding, the side chain of His 57 must be deprotonated, whereas the amino terminus (Ile 16) of the thrombin B chain should remain protonated in order to participate in a salt bridge with the side chain of Asp194 of thrombin. Disruption of this salt bridge by deprotonation of Ile 16 results in reduced binding affinity for fibrinogen. This model is based on the assumption that the fibrinogen substrate does not contain any amino acids with a pK_a value in the pH 6−10 range that would introduce further interactions in the system. These conditions are met only with the unphosphorylated peptide. Phosphorylation of FbgAα at the Ser3 position adds an amino acid with a pK_a in the 6.0 range and, therefore, may contribute a new factor into the model of Mathur et al. (*62*). Work by Betz et al. (*75*) indicated that the pH profile for the hirudin−thrombin complex contained a steeper drop in affinity at pHs greater than 8 than the rise in affinity at pHs less than 8. An amino acid residue of hirudin with a pK_a greater than 8 was proposed to participate in forming an efficient enzyme−substrate complex. Ser3P may introduce conditions in which the pH profile contains a greater rise in affinity at pH values less than 8 relative to that of the unphosphorylated peptide.

Examination of the Use of Phosphate in Regulating Enzyme Reactions. Although the biological function of phosphorylation of FbgAα at the Ser3 position is not known, phosphorylation is a modification that has been demonstrated to play a critical role in regulating numerous enzyme systems. Ser/Thr phosphoenzymes are often involved in intracellular processes and regulate enzyme function by an on/off switch mechanism using the phosphate group (*72*). Two enzymes in which the structural consequence of phosphorylation has been determined include mammalian/yeast glycogen phosphorylase and *Escherichia coli* isocitrate dehydrogenase (*71*, *76*). Tyr phosphoenzymes, by contrast, tend to be transmembrane proteins, and the phosphotyrosine functions as a recognition site for binding another target molecule (for example, SH2 domains) (*72*, *77*). On the basis of the results observed in this project, the phosphate group at the Ser3 position of FbgAα is proposed to play a role in mediating interactions with thrombin that is similar to that observed for Tyr phosphoenzymes.

There are several examples in which thrombin utilizes an anionic species as a linker molecule to bind another target protein. The negatively charged glucosaminoglycan heparin links antithrombin III to the thrombin anion-binding exosite II (reviewed in refs *78* and *79*). The C-terminal portion of hirudin involving amino acids 55−65 contains four glutamic acids and a tyrosine at position 63 that can be sulfated (*80*, *81*). This stretch of hirudin binds to thrombin through the anion binding exosite I (*78*, *79*, *82*) [also known as the fibrinogen recognition site]. Heparin cofactor II has also been shown to bind to exosite I with the aid of several different anionic species. Some examples include heparin,

polyphosphate, polyglutamate, and the phosphoserine glycoprotein phosvitin (*83*−*85*). FbgAα Ser3P may interact with thrombin through a salt bridge involving a neighboring Lys or Arg of the enzyme. Under conditions of physiological stress (surgery or pregnancy), the body may rely on FbgAα Ser3P to promote further interactions with the thrombin surface and/or to promote interactions with other portions of the FbgAα chain molecule.

Proposed Acceptor Sites on Thrombin for the Binding of FbgAα(1−*5 Ser3P).* To explore a possible binding site for Ser3P, solution structures for bound FbgAα(1−16 Ser3P) were docked onto the X-ray structure (*60*) of bovine thrombin− human FbgAα(7−16) using X-PLOR 3.1. The thrombin−FbgAα(1−16 Ser3P) complex was subjected to an energy minimization/simulated annealing protocol, keeping the X-ray structure of thrombin fixed. As can be seen in Figure 8, the Ser 3P side chain is positioned near a basic cluster of arginines and lysines. Depending upon the peptide structure chosen for docking, the Ser3P could bind with different orientations but (after the calculation in the presence of thrombin) it usually lay within the same thrombin environment; i.e., the phosphate group was found most often (to the extent of 66%) near thrombin R175 or K97.

The basic residues of bovine thrombin highlighted in Figure 8 form part of the rim of the thrombin heparin binding site (*78*). The heparin binding site is composed of a surface patch of positively charged side chains (K126, K236, K240, and R93) surrounded by the basic residues (R101, R233, R165, K169, K235, R175, R173, and K97). The site produces a strong positive electrostatic field and there is no evidence that the site contains fixed solvent anions (*78*). For the complex shown in Figure 8, the shortest average distance between the η protons on the R175 side chain and the oxygens on the serine phosphate was 5 Å. Torsional rotation of the Ser3 side chain could bring the distance down further to 2.0−2.7 Å. Within this distance range, the electrostatic interactions between the enzyme and peptide side chains should be significant. To be able to compare the structural results from this project with the NMR work of Ni et al. (*37*, *63*, *64*) and the X-ray studies of Martin et al. (*60*), complexes composed of bovine thrombin and human FbgAα-(1−20 Ser3P) were examined. Phosphorylated bovine fibrinopeptides, however, have not been observed in nature, and the physiological effects of such a modification are not known (*28*, *35*, *36*). This absence is not likely to be due to differences in the structure of bovine thrombin versus human thrombin. Bovine thrombin exhibits 87% identical residues with human thrombin and both contain the distinctive heparin binding site (*78*). The only sequence differences in the heparin binding site are switches from a Lys in bovine to an Arg in human thrombin for positions 126 and 97. The side chains on these amino acids have changed, but the positive, basic character has been conserved. On the basis of the NMR and docking studies carried out for this project, we propose that the phosphoserine at position 3 of the human FbgAα chain may interact with a basic residue in the heparin binding site, exosite II, thereby anchoring FbgAα(1−5) onto the thrombin surface. The phosphoserine is therefore hypothesized to function as another anionic linker to regulate interactions between thrombin and substrate/inhibitors.

CONCLUSIONS

In this work, we have shown that phosphorylation at the Ser3 position promotes new interactions between FbgAα-(1−20) and the thrombin surface. Kinetic studies indicate that this modification increases the substrate binding of fibrinogen Aα-like peptides toward thrombin. Phosphorylation, therefore, may play a role in producing a catalytically more efficient enzyme−substrate complex for the highly regulated blood coagulation system. ^{31}P and ^{1}H NMR studies reveal that introduction of a Ser3P allows FbgAα(1−5) to come in contact with the thrombin surface. This N-terminal segment of the Aα chain is proposed to be flexible and thus capable of anchoring to thrombin at the most accessible positively charged surface of the enzyme. The Ser3P is proposed to interact at the heparin binding region with the phosphate group, functioning as an anionic linker molecule.

ACKNOWLEDGMENT

We thank C. C. Lester for NMR technical advice and R. W. Sherwood for quantitative amino acid analysis. We also appreciate helpful discussions with E. E. DiBella.

REFERENCES

1. Halkier, T. (1991) *Mechanisms in Blood Coagulation, Fibrinolysis, and the Complement System*, pp 1−127, Cambridge, University Press, Cambridge, England.
2. Scheraga, H. A., and Laskowski, M., Jr. (1957) *Adv. Protein Chem. 12*, 1−131.
3. Lorand, L. (1951) *Nature 167*, 992−993.
4. Lorand, L., and Middlebrook, W. R. (1952) *Biochem. J. 52*, 196−199.
5. Lorand, L., and Middlebrook, W. R. (1952) *Biochim. Biophys. Acta 9*, 581−582.
6. Bettelheim, F. R., and Bailey, K. (1952) *Biochim. Biophys. Acta 9*, 578−579.
7. Bettelheim, F. R. (1956) *Biochim. Biophys. Acta 19*, 121−130.
8. Blomback B., and Vestermark, A. (1958) *Ark. Kemi 12*, 173−182.
9. Blomback, B., Blomback, M. Edman, P., and Hessel, B. (1966) *Biochim. Biophys. Acta 115*, 371−396.
10. Laudano A. P., and Doolittle, R. F. (1980) *Biochemistry 19*, 1013−1019.
11. Laki, K., and Lorand, L. (1948) *Science 108*, 280.
12. Lorand, L. (1952) *Biochem. J. 52*, 200−203.
13. Loewy, A. G., Dunathan, K., Kriel, R., and Wolfinger, H. L., Jr. (1961) *J. Biol. Chem. 236*, 2625−2633.
14. Lorand, L., Konishi, K., and Jacobsen, A. (1962) *Nature 194*, 1148−1149.
15. Scheraga, H. A. (1983) *Ann. N.Y. Acad. Sci. 408*, 330−343.
16. Scheraga, H. A. (1986) *Ann. N.Y. Acad. Sci. 485*, 124−133.
17. Blomback, B., Blomback, M., Edman, P., and Hessel, B. (1962) *Nature 193*, 883−884.
18. Seydewitz, H. H., Kasier, C., Rothweiler, H., and Witt, I. (1984) *Thromb. Res. 33*, 487−498.
19. Heldin, P., and Humble, E. (1987) *Arch. Biochem. Biophys. 252*, 49−59.
20. Humble, E., Heldin, P., Forsberg, P.-O., and Engström, L. (1985) *Arch. Biochem. Biophys. 241*, 225−231.
21. Forsberg, P.-O. (1989) *Thromb. Res. 53*, 1−9.
22. Sonka, J., Kubler, D., and Kinzel, V. (1989) *Biochim. Biophy. Acta 997*, 268−277.
23. Martin, S. C., Ekman, P., Forsberg, P.-O, and Ersmark, H. (1992) *Thromb. Res. 68*, 467−473.
24. Seydewitz, H. H., and Witt, I. (1985) *Thromb. Res. 40*, 29−39.
25. Witt, I., and. Müller, H. (1970) *Biochim. Biophy. Acta 221*, 402−404.

26. Martin, S. C., and Björk, I. (1990) *FEBS Lett. 272*, 103−105.
27. Martin, S. C., Forsberg, P.-O., and Eriksson, S. D. (1991) *Thromb. Res. 61*, 243−252.
28. Blömback, B., Blömback, M., and Searle, J. (1963) *Biochim. Biophys. Acta 74*, 148−151.
29. Martinelli, R. A., and Scheraga, H. A. (1980) *Biochemistry 19*, 2343−2350.
30. Kehl, M., Lottspeich, F., and Henschen, A (1981) *Hoppe-Seyler's Z. Physiol. Chem. 362*, 1661−1664.
31. Henschen, A., Lottspeich, F., Kehl, M., and Southan, C. (1983) *Ann. N.Y. Acad. Sci. 408*, 28−43.
32. Henschen, A., and McDonagh, J. (1986) in *Blood Coagulation* (Zwaal, R. F. A., and Hemker, H. C., Eds.) pp 171−241, Elsevier, Amsterdam.
33. Binnie, C. G., and Lord, S. T. (1993) *Blood 81*, 3186−3192.
34. Binnie, C. G., Hettasch, J. M., Strickland, E., and Lord, S. T. (1993) *Biochemistry 32*, 107−113.
35. Kudryk, B., Okada, M., Redman, C. M., and Blomback, B. (1982) *Eur. J. Biochem. 125*, 673−682.
36. Lucas, J., and Henschen, A. (1986) *J. Chromatogr. 369*, 357−364.
37. Ni, F., Konishi, Y., Frazier, R. B., Scheraga, H. A., and Lord, S. T. (1989) *Biochemistry 28*, 3082−3094.
38. Hanna, L. S., Scheraga, H. A., Francis, C. W., and Marder, V. J. (1984) *Biochemistry 23*, 4681−4687.
39. Perich, J. W. (1992) *Int. J. Pept. Protein Res. 40*, 134−140.
40. Andrews, D. M., Kitchin, J., and Seale, P. W. (1991) *Int. J. Pept. Protein Res. 38*, 469−475.
41. Winzor, D. J., and Scheraga, H. A. (1964) *Arch. Biochem. Biophys. 104*, 202−207.
42. DiBella, E. E., and Scheraga, H. A. (1996) *Biochemistry 35*, 4427−4433.
43. Bevington, P. R. (1969) in *Data Reduction and Error Analysis for the Physical Sciences*, pp 92−118, McGraw-Hill, New York.
44. Marquardt, D. W. (1963) *J. Soc. Ind. Appl. Math. 11*, 431−441.
45. Hwang, T.-L., and Shaka, A. J. (1995) *J. Magn. Reson. Ser. A, 112*, 275−279.
46. Wüthrich, K. (1986) *NMR of Proteins and Nucleic Acids*, pp 1−161, John Wiley and Sons, New York.
47. Ni, F., Scheraga, H. A., and Lord, S. T. (1988) *Biochemistry 27*, 4481−4491.
48. Campbell A. P., and Sykes, B. D. (1993) *Annu. Rev. Biophys. Biomol. Struct. 22*, 99−122.
49. Ni, F., and Scheraga, H. A. (1994) *Acc. Chem. Res. 27*, 257−264.
50. Ni, F. (1994) *Prog. NMR Spectrosc. 26*, 517−606.
51. Clore, G. M., and Gronenborn, A. M. (1982) *J. Magn. Reson. 48*, 402−417.
52. Clore, G. M., and Gronenborn, A. M. (1983) *J. Magn. Reson. 53*, 423−442.
53. Gorenstein, D. G. (1984) *Phosphorous-31 NMR. Principles and Applications*, pp 7−154, Academic Press, Orlando, FL.
54. Brunger, A. T. (1992) *X-PLOR Version 3.1 User Manual*, Yale University Press, New Haven, CT.
55. Powell, M. J. D. (1977) *Math. Program. 12*, 241−254.
56. Nilges, M., Clore, G. M., and Gronenborn, A. M. (1988) *FEBS Lett. 229*, 317−324.
57. Nilges, M., Clore, G. M., and Gronenborn, A. M. (1988) *FEBS Lett. 239*, 129−136.
58. Nilges, M., Clore, G. M., and Gronenborn, A. M. (1990) *Biopolymers 29*, 813−822.
59. Byeon, I.-J. L., Kelley, R. F., Mulkerrin, M. G, An, S. S. A., and Llinás, M. (1995) *Biochemistry 34*, 2739−2750.
60. Martin, P. D., Robertson, W., Turk, D., Huber, R., Bode, W., and Edwards, B. F. P. (1992) *J. Biol. Chem. 267*, 7911−7920.
61. Marsh, H. C., Meinwald, Y. C., Thannhauser, T. W., and Scheraga, H. A. (1983) *Biochemistry 22*, 4170−4174.
62. Mathur, A., Schlapkohl, W. A., and Di Cera, E. (1993) *Biochemistry 32*, 7568−7573.
63. Ni, F., Zhu, Y., and Scheraga, H. A. (1995) *J. Mol. Biol. 252*, 656−671.
64. Ni, F., Meinwald, Y. C., Vásquez, M., and Scheraga, H. A. (1989) *Biochemistry 28*, 3094−3105.
65. Zheng, Z., Ashton, R. W., Ni, F., and Scheraga, H. A. (1992) *Biochemistry 31*, 4426−4431.
66. Güntert, P., Braun, W., and Wüthrich, K. (1991) *J. Mol. Biol. 217*, 517−530.
67. Güntert, P., Qian, Y. Q., Otting, G., Müller, M., Gehring, W., and Wüthrich, K. (1991) *J. Mol. Biol. 217*, 531−540.
68. Güntert, P., and Wüthrich, K. (1991) *J. Biomol. NMR 1*, 447−456.
69. Humphrey, R. S., and Jolley, K. W. (1982) *Biochim. Biophys. Acta 708*, 294−299.
70. Hoffman, R., Reichert, I., Wachs, W. O., Zeppezauer, M., and Kalbitzer, H. R. (1994) *Int J. Pept. Protein Res. 44*, 193−198.
71. Johnson, L. N., and Barford, D. (1994) *Protein Sci. 3*, 1726−1730.
72. Mavri, J., and Vogel, H. J. (1996) *Proteins: Struct., Funct., Genet. 24*, 495−501.
73. Sturtevant, J. M., Laskowski, M., Jr., Donnelly, T. H., and Scheraga, H. A. (1955) *J. Am. Chem. Soc. 77*, 6168−6172.
74. Endres, G. F., Ehrenpreis, S., and Scheraga, H. A. (1966) *Biochemistry 5*, 1561−1567.
75. Betz, A., Hofsteenge, J., and Stone, S. R. (1992) *Biochemistry 31*, 1168−1172.
76. Lin, K. Rath, V. L., Dai, S. C., Fletterick, R. J., and Hwang, P. K. (1996) *Science 273*, 1539−1541.
77. Pawson, T., and Gish, G. D. (1992) *Cell 71*, 359−362.
78. Bode, W., Turk, D., and Karshikov, A. (1992) *Protein Sci. 1*, 426−471.
79. Stubbs, M. T., and Bode, W. (1993) *Thromb. Res. 69*, 1−58.
80. Bagdy, D., Barabas, E., Graf, L., Petersen, T. E., and Magnusson, S. (1976) *Methods Enzymol. 45*, 669−678.
81. Dodt, J., Seemuller, U., Maschler, R., and Fritz, H. (1985) *Biol. Chem. Hoppe-Seyler 366*, 379−385.
82. Rydel, T. J., Ravichandran K. G., Tulinsky, A., Bode, W., Huber, R., Roitsch, C., and Fenton, J. W., II (1990) *Science 249*, 277−280.
83. Church, F. C., Pratt, C. W., Treanor, R. E., and Whinna, H. C. (1988) *FEBS Lett. 237*, 26−30.
84. Rogers, S. J., Pratt, C. W., Whinna, H. C., and Church, F. C. (1992) *J. Biol. Chem. 267*, 3613−3617.
85. Melton, L. G., Church, F. C., and Erickson, B. W. (1995) *Int. J. Pept. Protein Res. 45*, 44−52.

BI972538W